Frequency Tunable Microstrip Patch Antenna Using RF MEMS Technology

Emre Erdil, Kagan Topalli, Mehmet Unlu, Ozlem Aydin Civi, and Tayfun Akin

***Abstract*—A novel reconfigurable microstrip patch antenna is presented that is monolithically integrated with RF microelectromechanical systems (MEMS) capacitors for tuning the resonant frequency. Reconfigurability of the operating frequency of the microstrip patch antenna is achieved by loading it with a coplanar waveguide (CPW) stub on which variable MEMS capacitors are placed periodically. MEMS capacitors are implemented with surface micromachining technology, where a 1-μm thick aluminum structural layer is placed on a glass substrate with a capacitive gap of 1.5 μm. MEMS capacitors are electrostatically actuated with a low tuning voltage in the range of 0–11.9 V. The antenna resonant frequency can continuously be shifted from 16.05 GHz down to 15.75 GHz as the actuation voltage is increased from 0 to 11.9 V. These measurement results are in good agreement with the simulation results obtained with Ansoft HFSS. The radiation pattern is not affected from the bias voltage. This is the first monolithic frequency tunable microstrip patch antenna where a CPW stub loaded with MEMS capacitors is used as a variable load operating at low dc voltages.**

***Index Terms*—Microelectromechanical system (MEMS), microstrip antennas, microwave, reconfigurable architectures.**

I. Introduction

Microelectromechanical systems (MEMS) and the application of this technology to RF systems enable production of tunable components with low power consumption, high linearity and high performance. The tunable characteristics of RF MEMS are employed in the integration of these components with antennas providing numerous advantages such as reconfigurability in the polarization, frequency, and radiation pattern [1]. Furthermore, the monolithic fabrication of the antenna together with these tunable components reduces the power losses and parasitic effects compared to integration of discrete components. It has been shown in literature that MEMS switches and MEMS tunable capacitors are used in reconfigurable antennas to control the resonant frequency, bandwidth, polarization, and radiation pattern of these antennas [2]–[4].

This paper presents a novel tunable frequency microstrip patch antenna using the RF MEMS technology. The structure consists of a patch antenna loaded with a coplanar waveguide (CPW) loading section attached to the antenna via microstrip to CPW transition. The reconfigurability in the resonant frequency of the antenna is provided with the aid of the MEMS bridges acting as a variable capacitor placed on the CPW stub. The structure is designed and simulated with Ansoft HFSS v9.2, and it is fabricated using the surface micromachining process developed at the Microelectronics Facilities of Middle East Technical University. Measurement results verify the change in the resonant frequency of the antenna with low actuation voltages.

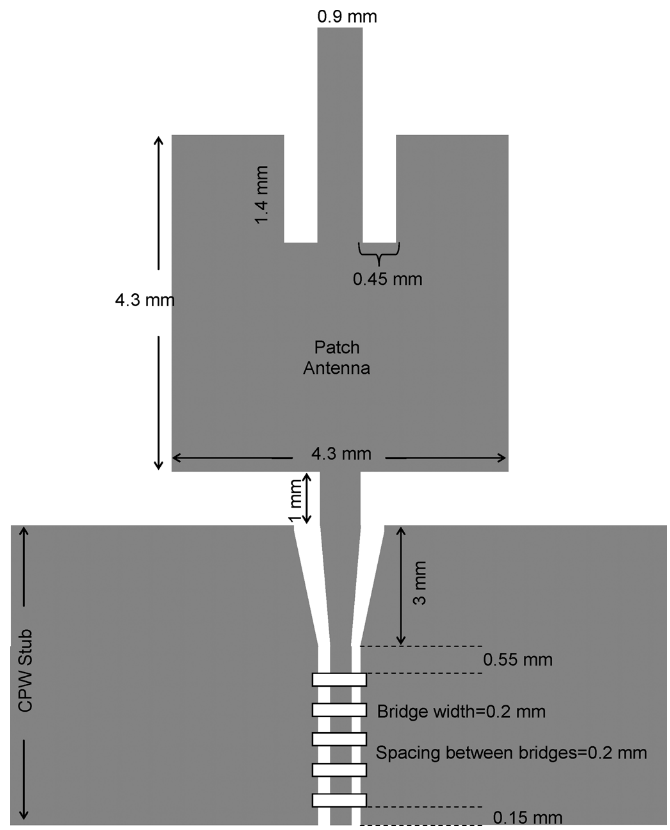

Fig. 1. Schematic view of the frequency tunable microstrip patch antenna.

II. Antenna Design

Fig. 1 shows the schematic view of the frequency tunable microstrip antenna. The structure employs the idea of loading one of the radiating edges of the microstrip patch antenna with a CPW stub on which RF MEMS bridge type capacitors are placed periodically. The height of the bridges on the stub, hence the loading capacitance, can be changed by the dc actuation voltage applied between the center conductor and MEMS bridge metal. Thus, the CPW stub with bridges provides a variable load to the radiating edge that is connected, resulting in tunability in the resonant frequency. In order to integrate the CPW stub with the antenna, a microstrip line section and a tapered line are used for a proper transition.

III. Fabrication

The antenna structure presented in this work is fabricated using the standard surface micromachining process developed at METU for implementation of various RF MEMS components on 500 μm-thick Pyrex 7740 glass substrate ($\varepsilon_r = 4.6$, $\tan\delta = 0.005$). The process starts with sputtering of 100/3000 Å-thick Ti/Au, which is required as the seed layer for electroplating of gold layer. A 2-μm thick gold layer is electroplated inside the regions defined by the mold SPR 220-3 photoresist. The remaining Ti/Au seed layer is etched using wet etching with selective titanium and gold etchants. A 3000-Å thick Si_3N_4 layer is coated as the dc isolation layer using plasma enhanced chemical vapor deposition technique (PECVD) and patterned using the reactive ion etching (RIE) technique. The next step is the spin-coating of the

Manuscript received June 5, 2006; revised December 4, 2006. This work was supported in part by The Scientific and Technical Research Council of Turkey (TUBITAK-EEEAG-102E036-COST284), in part by the Turkish State Planning Organization (DPT), and in part by the Advanced MEMS For RF and Millimeter Wave Communications (AMICOM) Network of Excellence under 6th Framework Program of European Union.

E. Erdil is with the Department of Information Technology, Capital Markets Board of Turkey, Ankara 06530, Turkey.

K. Topalli, M. Unlu, O. A. Civi, and T. Akin are with the Department of Electrical and Electronics Engineering, Middle East Technical University, Ankara 06531, Turkey (e-mail: kagan@metu.edu.tr).

Color versions of one or more of the figures in this paper are available online at http://ieeexplore.ieee.org.

Digital Object Identifier 10.1109/TAP.2007.893426

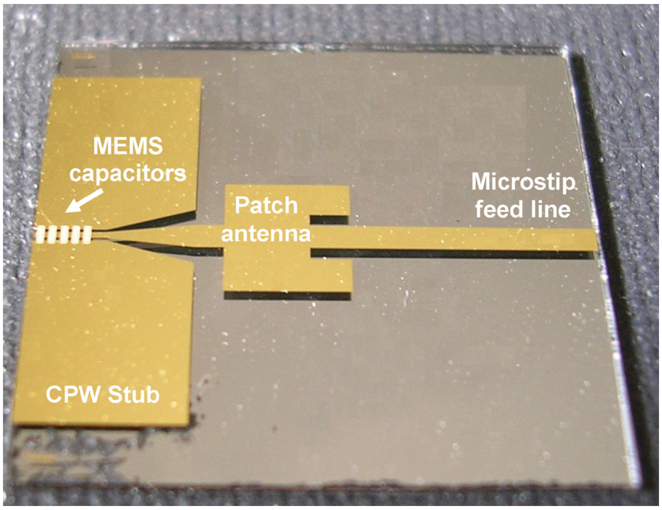

Fig. 2. Photograph of the fabricated antenna structure.

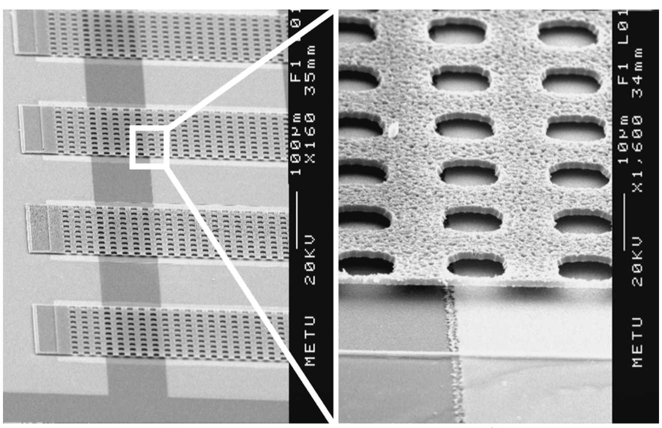

(a) (b)

Fig. 3. (a) SEM photograph of the loading section of the frequency tunable antenna and (b) detailed view of the bridge region marked in (a).

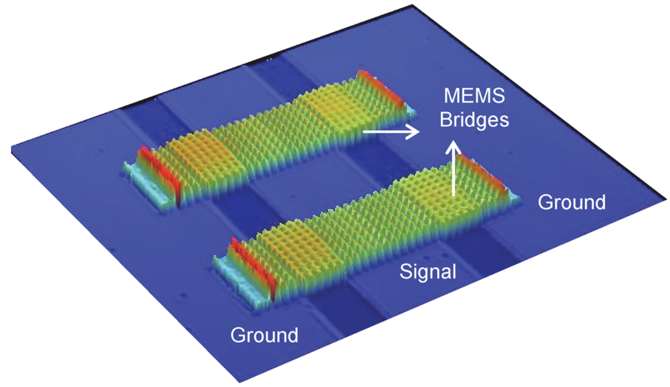

Fig. 4. Light-interferometer microscope view of two MEMS bridges with a height of 1.4 μm around the center conductor of CPW loading section.

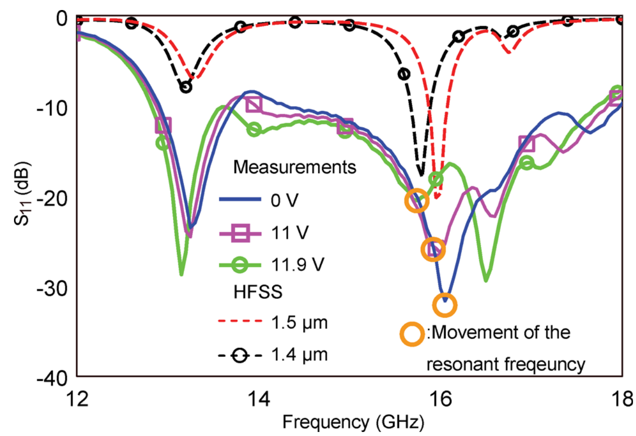

Fig. 5. Reflection coefficient characteristics for different actuation voltages and simulation results.

photodefinable polyimide, PI2737, as the 1.5-μm thick sacrificial layer. Then, a 1-μm thick aluminum layer is sputter-deposited and patterned as the structural layer. Finally, the structures are released after dry-etching of the sacrificial layer in O_2 plasma.

IV. Measurements and Conclusions

Fig. 2 shows the photograph of the fabricated antenna structure. Fig. 3 presents the SEM photographs of the MEMS capacitors on the loading section of the patch antenna. The RF measurements of the antenna are performed using the HP 8720 D 0.05–20 GHz vector network analyzer. The picosecond 5542-230 bias-tee attached to the antenna connector is used to apply both polarities of the actuation voltage, where the positive polarity is applied to the center conductor of the CPW via the microstrip line, while the other polarity is supplied to the ground planes of CPW by shorting plates at the edge of the CPW stub connecting the upper and lower grounds to provide dc short. The height of the MEMS capacitors when there is no bias is measured with the light-interferometer microscope. Fig. 4 gives the 3-D plot of the surface profile data obtained by the microscope. The height of the MEMS bridges around the center conductor is found to be 1.5 μm. Fig. 5 shows the reflection coefficient characteristics of the antenna structure for different actuation voltages applied to the MEMS bridges. The resonant frequency around 16.05 GHz shifts down to 15.75 GHz as the actuation voltage is increased from 0 to 11.9 V, where the height of the capacitive gap changes from 1.5 μm to 1.4 μm. The other resonant behavior is observed around 13.2 GHz due to the loading of the CPW stub to the patch antenna. Measurements and EM simulations show resonances at the same frequencies for the same actuation voltages and capacitive gaps for the 12–18 GHz band. During the HFSS simulations, an air box covering the whole structure is defined in order to include the fringe fields of the open-ended CPW. The dc connection between the top and bottom plates does not have a significant effect on the performance since it is connected at the edge of the CPW stub on which the fields are concentrated only around the gaps of the CPW line and bridges. It should be noted here that all metal layers in the simulations have finite thickness and finite conductivity. The conductivity of the metal layers which depends on the processing conditions is measured to be between 2.5×10^7 S/m and 2.8×10^7 S/m. In the simulations, the conductivity is assumed to be 2.5×10^7 S/m. The discrepancy between the amplitudes of the reflection coefficients in the simulations and measurements can be explained as an effect of SMA connector used in the measurements, but not taken into account during simulations. The effect of SMA connector has been verified with the two-port measurements of a microstrip line on a glass substrate fabricated with the same process. Due to the discontinuity at the transition from the coaxial line to microstrip trace, which can be modeled as a series inductor and a shunt capacitance, the measurement with the connectors shows significant

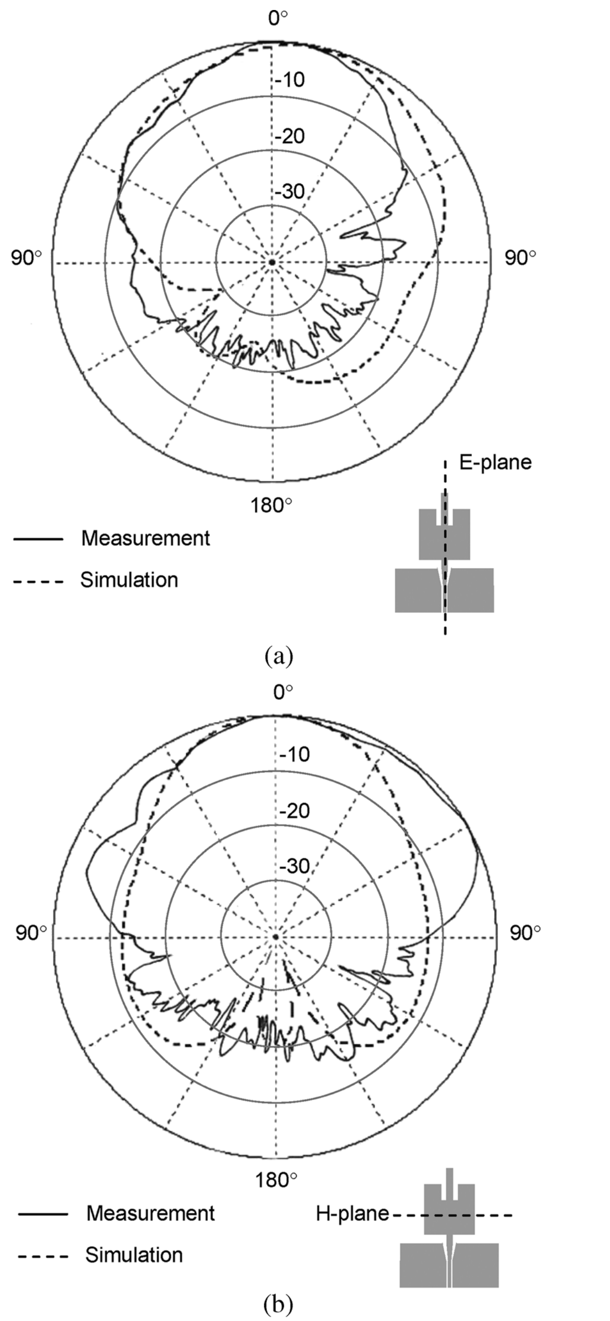

Fig. 6. Simulated and measured radiation pattern of the antenna when the switches are at the up position. (a) E-plane pattern and (b) H-plane pattern.

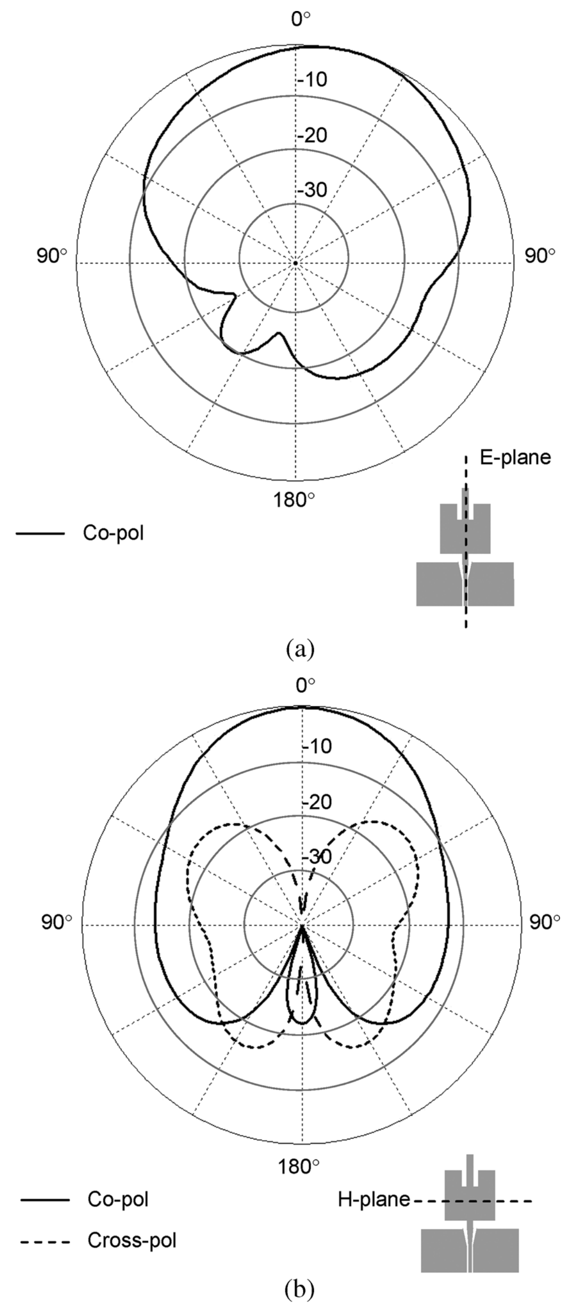

Fig. 7. Simulated pattern of the antenna at 15.75 GHz when the dc bias is applied (1.4 $\mu\mathrm{m}$ bridge height). (a) E-plane. (b) H-plane. The cross-polarization level in E-plane is not shown since it is lower than 40 dB.

amount of deviation compared to the simulations of the microstrip line without SMA connectors particularly at frequencies higher than 10 GHz. The difference in the transmission coefficient characteristics is about 4–5 dB at the *Ku*-band. The effects of the discontinuity due to SMA connector can be compensated with the use of stubs on the feed line of the antenna. Since the aim of this work is to show the tuning of the resonant frequency of the antenna by MEMS capacitors, compensation study to reduce the effects of the connector is not performed in the frame of this work.

Fig. 6 shows the simulated and measured radiation pattern of the antenna at 16.05 GHz when the switches are at the up position. The simulation and measurement results are in good agreement for both E- and H-planes. The asymmetry and the tilted maximum radiation in the E-plane are expected as the feed line and the dimensions of loading stub are considered. Fig. 7 gives simulated radiation pattern when the bridges are lowered down to 1.4 $\mu\mathrm{m}$ to simulate the case under dc actuation. The radiation pattern of the antenna is not affected from the change of the resonant frequency with dc voltage.

V. Conclusion

This work shows a frequency tunable microstrip patch antenna where a CPW stub loaded with MEMS capacitors is used. The electrical length of the stub is adjusted as the MEMS capacitors are controlled via dc actuation voltage. This variable stub provides a frequency shift of 300 MHz without distorting the radiation pattern under dc bias. The capacitor type used in the design is a fixed-fixed beam capacitor design with a tuning range limited by the pull-in instability. The tuning range of the antenna can be increased either by increasing the tuning range of the MEMS capacitors [5] or by the use of variable capacitors at different places on both of the radiating edges to load the antenna [6]. However both of these approaches can be achieved at the expense of an increase in the dc biasing and fabrication complexity. Although the CPW stub increases the antenna dimension significantly, it is a simple way of loading a patch antenna with a standard MEMS fabrication process. The dimensions of CPW grounds are intentionally increased to obtain a proper transition without using any via hole between CPW ground and microstrip ground. This is a proof of concept type work. The experience gained in this work is important in terms of showing the potential application of MEMS technology to implement reconfigurable architectures. Recently, this concept is applied to a more compact antenna structure [7].

ACKNOWLEDGMENT

The authors would like to thank the staff of Middle East Technical University, Microelectronics Facilities (METU-MET) for their support in the fabrication.

REFERENCES

[1] G. M. Rebeiz, *RF MEMS Theory, Design, and Technology*. Hoboken, NJ: Wiley, 2003.

[2] R. N. Simons, D. Chun, and L. P. B. Katehi, "Microelectromechanical systems (MEMS) actuators for antenna reconfigurability," in *IEEE MTT-S Int. Microwave Symp. Digest*, May 2001, pp. 215–218.

[3] ——, "Polarization reconfigurable patch antenna using Microelectromechanical Systems (MEMS) actuators," in *IEEE AP-S Symp. Digest*, Jun. 2002, pp. 6–9.

[4] J. C. Chiao, S.-Y. Cheng, J. L. Chang, I. M. Chio, Y. Kang, and J. Hayasaka, "MEMS reconfigurable antennas," *Int. J. RF Microwave CAE*, vol. 11, pp. 301–309, 2001.

[5] D. Peroulis and L. P. B. Katehi, "Electrostatically-tunable analog RF MEMS varactors with measured capacitance range of 300%," in *IEEE MTT-S Int. Microwave Symp. Digest*, 2003, pp. 1793–1796.

[6] Z. Jin and A. Mortazawi, "An L-band tunable microstrip antenna using multiple varactors," in *IEEE AP-S Symp. Digest*, 2003, pp. 524–527.

[7] E. Erdil, K. Topalli, M. Unlu, I. Istanbulluoglu, E. U. Temocin, H. I. Atasoy, O. Bayraktar, O. A. Civi, S. Demir, S. Koc, and T. Akin, "Reconfigurable slot antenna with fixed-fixed beam type RF MEMS capacitors," in *Proc. Eur. Conf. on Antennas and Propagation*, Nov. 6–10, 2006, on CD.

Wideband Microstrip Patch Antenna With U-Shaped Parasitic Elements

Sang-Hyuk Wi, Yong-Shik Lee, and Jong-Gwan Yook

***Abstract*—A wideband U-shaped parasitic patch antenna is proposed. Two parasitic elements are incorporated into the radiating edges of a rectangular patch whose length and width are $\lambda_g/2$ and $\lambda_g/4$, respectively, in order to achieve wide bandwidth with relatively small size. Coupling between the main patch and U-shaped parasitic patches is realized by either horizontal or vertical gaps. These gaps are found to be the main factors of the wideband impedance matching. The proposed antenna is designed and fabricated on a small size ground plane (25 mm $\times$ 30 mm) for application of compact transceivers. The fabricated antenna on a FR4 substrate shows an impedance bandwidth of 27.3% (1.5 GHz) at 5.5 GHz center frequency. The measured radiation patterns are similar to those of a conventional patch antenna with slightly higher gains of 6.4 dB and 5.2 dB at each resonant frequency.**

***Index Terms*—Parasitic patch antenna, U-shaped parasitic patches, wide bandwidth.**

I. INTRODUCTION

Demand for compact and multifunctional wireless communication systems has spurred the development of multiband and wideband antennas with small size. Microstrip patch antennas are widely used in this regard as they offer compactness, a low profile, light weight, and economical efficiency. However, the microstrip patch antenna is limited by its narrow operating bandwidth.

There are numerous and well-known methods to increase the bandwidth of antennas, including increase of the substrate thickness [1], the use of a low dielectric substrate [1], the use of various impedance-matching and feeding techniques [2], the use of multiple resonators [3]–[7], and the use of slot antenna geometry [8]. However, the bandwidth and the size of an antenna are generally mutually conflicting properties, that is, improvement of one of the characteristics normally results in degradation of the other.

Recently, several techniques have been proposed to enhance the bandwidth. In [9]–[11], utilizing the shorting pins or shorting walls on the unequal arms of a U-shaped patch, U-slot patch, or L-probe feed patch antennas, wideband and dual-band impedance bandwidth have been achieved with electrically small size.

In this work, a wideband microstrip patch antenna employing parasitic elements is investigated. Two U-shaped parasitic elements are incorporated along the radiating edges of a probe fed rectangular patch antenna so as to obtain wideband operating frequency. In addition, the antenna is relatively small in comparison with the conventional parasitic patch antenna described in [4], [5]. Performance of the proposed antenna is calculated and measured. The proposed antenna geometry is described in Section II. The fabricated antenna and experimental validations are presented in Section III.

Manuscript received August 2, 2006; revised October 11, 2006. This work was supported by the Ministry of Information and Communication (MIC), Korea, under the Information Technology Research Center (ITRC) support program supervised by the Institute of Information Technology Assessment (IITA-2005-C1090-0502-0012).

The authors are with the Department of Electrical and Electronic Engineering, Yonsei University, Seoul 120-749, Korea (e-mail: wshnury@yonsei.ac.kr; jgyook@yonsei.ac.kr).

Digital Object Identifier 10.1109/TAP.2007.893427